Surface modification of PCL-TCP scaffolds in rabbit calvaria defects: Evaluation of scaffold degradation profile, biomechanical properties and bone healing patterns

Alvin Yeo,[1,2,3] Wah Jie Wong,[3] Swee-Hin Teoh[3,4]
[1]*Department of Restorative Dentistry, National Dental Centre, SingHealth, Singapore*
[2]*Department of Orthodontics, University of Groningen, Netherlands*
[3]*Department of Mechanical Engineering, National University of Singapore, Singapore*
[4]*National University of Singapore Tissue Engineering Programme (NUSTEP), National University of Singapore, Singapore*

Received 6 March 2009; revised 29 May 2009; accepted 20 July 2009
Published online 12 November 2009 in Wiley InterScience (www.interscience.wiley.com). DOI: 10.1002/jbm.a.32633

Abstract: Traditionally, polycaprolactone (PCL) based scaffolds tend to degrade at a slow rate. Pretreatment of polycaprolactone-20% tricalcium phosphate (PCL-TCP) scaffolds under alkaline conditions can be utilized to increase the degradation rate and improve mechanical properties. Three groups of PCL-TCP scaffolds with varying pretreatment exposures with sodium hydroxide (NaOH) were studied in a rabbit calvaria defect model and analyzed at 2, 4, 8, 12, and 24 weeks. (Group A: Untreated, Group B: 3 *M* NaOH/48 h and Group C: 3 *M* NaOH/96 h). Micro-CT analysis demonstrated that scaffolds with increased surface roughness (Groups B and C) showed a greater impact on the overall volume loss during the early healing period between 2 and 8 weeks as compared to the untreated group. In addition, greater bone formation was detected in NaOH treated scaffolds as compared to the untreated group throughout the experiment. Scaffolds with increased surface roughness generally reported higher push out test and compressive strength values from 4 to 8 weeks of early healing. Interestingly, the mechanical properties displayed a decline in values from 12 weeks onwards in the modified groups suggesting a favorable breakdown or weakening of PCL-TCP scaffolds tailored for replacement by new bone formation. © 2009 Wiley Periodicals, Inc. J Biomed Mater Res 93A: 1358–1367, 2010

Key words: polycaprolactone; scaffold; degradation; bone; surface modification

INTRODUCTION

PCL-TCP scaffolds have been extensively studied and demonstrated excellent results in bone tissue engineering applications.[1–6] Previous studies have shown that these scaffolds with 70–75% porosity values possess many of the desired characteristics for use as a biodegradable scaffold; however due to the high molecular weight and hydrophobic nature, polycaprolactone-based scaffolds generally tend to degrade at a slow rate.[7,8] When indicated for dentoalveolar reconstruction, scaffolds should degrade predictably over an optimal period of 5–6 months whilst maintaining structural support and allowing new bone formation to occur and replace accordingly.[9,10] This is often followed by the insertion of dental implants and thereafter a final dental prosthesis.

There has been an increasing trend for researchers to modify the surface characteristics and architecture of scaffolds used for tissue engineering. It has been shown that improved osteoconductivity of a biomaterial could be achieved if the microstructure roughness could be enhanced.[11,12] Greater osteoblast adhesion and function and increased levels extracellular matrix proteins were reported on surfaces with higher surface roughness.[13–15] Particle and pore size geometry are important characteristics of any scaffold or biomaterial.[8] It has been proposed that a smaller particle size and a larger pore configuration encouraged more rapid bioabsorption and enhanced osteogenesis through a greater surface area.[16] A

Correspondence to: S. H. Teoh; e-mail: mpetsh@nus.edu.sg
Contract grant sponsor: NMRC; contract grant number: 022/07-25380020
Contract grant sponsor: ExxonMobil-NUS Research Fellowship Award

recent study investigated the effects of scaffold surface characteristics on stem cell performance. Results showed conclusively that scaffold with increased surface roughness in the form of microcavities, exhibited a more robust osteogenic response as compared to smooth surface scaffolds.[17]

Our group has been actively testing and customizing a novel bioresorbable scaffold (80% PCL: 20% TCP) targeted for dentoalveolar applications. Earlier, we reported on the degradation profile of novel PCL-TCP scaffolds in an *in vitro* and *in vivo* environment. Although the degradation rate was accelerated with the addition of TCP particles, it was however still unfavorable after 6 months.[18] It had been demonstrated that our lab's fabricated PCL-TCP scaffolds produced favorable pore geometry of 400–600 μm and rod diameter of ~250 μm.[8,19] Our team proceeded to modify the PCL-TCP scaffolds with the intent to further increase the degradation rate and improve the surface characteristics by pretreating with lipase and sodium hydroxide (NaOH). Findings from our previous study reported that pretreatment of PCL-TCP scaffolds with NaOH can be used to improve surface characteristics, which can be tailored to encourage a more rapid degradation rate and in turn enhance early bone formation. In addition, these modified scaffolds were shown to retain favorable mechanical properties essential in withstanding moderate load-bearing forces, such as intraoral dentoalveolar applications.[20] Scanning electron images (SEM) and micro-computed tomography (micro-CT) results obtained from our most recent study demonstrated improved wettability of PCL-TCP scaffolds when treated with NaOH. This improved hydrophilicity of the treated scaffolds resulted in greater initial matrix deposition and promoted early bone ingrowth. A greater number and size of micro pits with "channel-like" indentations were detected after NaOH treatment. Interestingly, it did not affect the overall pore dimensions and interconnected honeycomb architecture even after 48 and 96 h of NaOH treatment.[21]

The aim of the present study was to investigate the effects of increased surface roughness of PCL-TCP scaffolds on the degradation profile, mechanical properties and new bone formation in a rabbit calvaria defect model over a period of 6 months. Mechanical analyzes, such as compression and push out testing were performed to evaluate the overall strength of the newly regenerated bone within the scaffold and the interfacial shear strength at the bone-scaffold interface respectively. The extent of loss of scaffold volume, new bone formation and the healing patterns were determined using micro-CT, histology and histomorphometry analyzes.

MATERIALS AND METHODS

Scaffold fabrication

Scaffold specimens were fabricated with PCL-20% TCP filaments using a fused deposition modeling (FDM) 3D Modeler RP system from Stratasys Inc (Eden Prairie, MN). Blocks of 50 × 50 × 2 mm were created directly in Stratasys Quickslice (QS) software. They were directly purchased from Osteopore International Pte, Singapore. A lay-down pattern of 0/60/120° was used to give a honeycomb-like pattern of triangular pores with a porosity of 75%. The specimens were then cut into smaller discs of 6mm in diameter and 2 mm in thickness.

Study design and alkaline treatment of scaffolds

Three groups of PCL-TCP scaffolds were analyzed:

A. Untreated.
B. 3 mol L^{-1} (3 *M*) NaOH treated/48 h.
C. 3 mol L^{-1} (3 *M*) NaOH treated/96 h.

PCL-TCP scaffolds in the treated groups B and C were immersed in phosphate buffer saline (PBS, 137 m*M* NaCl, 2.7 m*M* KCL, 10 m*M* Na_2HPO_4, 1.8 m*M* KH_2PO_4, pH 7.4) for 2 h followed by immersion into 3 *M* NaOH for 48 and 96 h at 37°C respectively. The treated scaffolds were then removed and rinsed in PBS three times. Scanning electron micrograph (SEM) images of NaOH treated PCL-TCP scaffolds at various time intervals are shown in Figure 1.

Experimental design

The scaffolds were randomly assigned to the defects made in the calvaria of rabbits and followed up for 2, 4, 8, 12, and 24 weeks. Micro-CT, mechanical strength testing

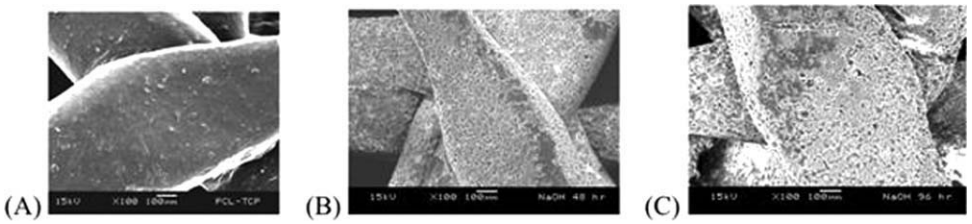

Figure 1. SEM images of PCL-TCP scaffolds treated with NaOH for (A) 0 h (B) 48 h (C) 96 h.

(compressive strength and push out test), histology analyzes were performed. A minimum of 11 samples are required for each experimental group at 2 weeks, 4 weeks (1 month), 8 weeks (2 months), 12 weeks (3 months), and 24 weeks (6 months) time points respectively to have sufficient data for analysis as recommended by ISO standard 10,993–6. Since we had a total of 33 samples at each time point and three samples were implanted in each rabbit, 55 rabbits were needed for the entire study.

Animal husbandry and scaffold implantation

Fifty-five, 6–8 month-old New Zealand White male rabbits were used. The study was approved by the SingHealth Institutional Animal Care and Use Committee (IACUC) and conformed to the respective guidelines. The rabbits were operated on under general anesthesia, which consisted of an intraperitoneal injection of ketamine and xylazine mixture (75 mg/kg + 10 mg/kg). Under anesthesia, the skull region of the rabbit was shaved and scrubbed with iodine, followed by disinfection with 70% ethyl alcohol.

A midline incision was made in the skin of the calvaria along the sagittal suture line. The soft tissue and periosteum are elevated and reflected. Under constant saline irrigation, 6 mm diameter circular and 2 mm deep defects were made using the appropriate trephine drills. A total of 3 circular defects were made on the calvarium of each rabbit. Care is taken to preserve the dura. Defects were randomly assigned to receive 1 of the 3 test scaffolds (Fig. 3). Prior closure, a nonresorbable membrane was positioned over the defects to prevent soft tissue ingrowth. This was followed by repositioning of the periosteum to cover the scaffolds followed by closure of the skin with sutures. The rabbits were then given carpofen (1–2 mg/kg) and cephalexin (15–20 mg/kg) subcutaneously for 3 and 5 days respectively.

Eleven rabbits were euthanized at 2, 4, 8, 12, and 24 weeks respectively. All samples were processed and analyzed accordingly. The tissues surrounding the selected implanted scaffolds were carefully removed and stored in 10% neutral buffered formalin (NBF) for histology ($n = 3$). The remaining samples were wrapped in PBS-soaked gauze and frozen at $-20^{\circ}C$ and subsequently subjected for micro-CT ($n = 4$; non-destructive), push out ($n = 4$), compressive strength testing ($n = 4$) analyzes. The rabbits were closely monitored everyday for the first week for presence of swelling, pain and infection. They were then observed weekly for severe weight loss (20–25%) and any other complications.

Mechanical strength testing

Compressive test

Two kinds of mechanical testing (compressive test and push out test) were performed using the Instron 5500 micro tester (Instron, Canton, MA) with a 1kN load cell. Each specimen was placed between two flat plates for compression testing. The scaffolds were compressed at a speed of 1 mm/min up to 80% of scaffold original thickness at room temperature. The mechanical results of load and extension were used to calculate the σ, compressive stress (MPa) = [load (N)/area (m^2)] $\times$ (1×10^{-6}); ε, strain = extension (mm)/original length (mm); and E, elastic modulus (MPa) = compressive stress (MPa)/strain. A stress–strain curve was then plotted using the experimental data (load versus deformation) and the compressive modulus and strength was recorded for each specimen, with the stiffness being measured as the slope of the linear portion of the curve.

Push out test

Utilizing a similar Instron 5500 micro tester, push out test was done using the same configuration except that a support jig with a hole of 7.2 mm was used (Fig. 2). Interfacial shear strength between old bone and the newly regenerated bone-scaffold composite was calculated by dividing peak force with cross sectional area of specimen.

Micro-CT analysis

Native and NaOH treated scaffolds were being isotropically scanned at 14 μm resolution with an SMX-100CT micro-CT scanner (Shimadzu, Japan) using a cone CT scanning technique. To ensure a consistent CT image resolution among all the datasets, the scanner turntable location was fixed at a specific source-to-object distance (SOD; 48.03 mm) and source-to-image distance (SID; 361.30 mm) respectively. X-ray parameters were set at 33 kV and 156 μA and the CT images were processed at a scaling coefficient of 100 and averaged three times. Region of interest (6 mm diameter) was drawn at the site of implantation. Resultant micro-CT datasets for each bone cube were evaluated for microarchitectural parameters using VG Studio Max software (Heidelberg, Germany). Overall bone formation and scaffold volume loss were obtained and analyzed.

Histological analysis

The specimens were removed and stored in NBF 4% and were dehydrated in ascending series of alcohol rinses and embedded using a process that produced ground sections with the glycol metacrylate resin. Once polymerized, the block is trimmed to remove excess plastic with an industrial vertical band saw and cut along its long axis with a diamond band saw (EXAKT standard saw). Ground polished sections of 10 μm thickness were made using the EXAKT micro grinder system (EXAKT Technologies, Oklahoma City, OK) and were subsequently stained with Hematoxylin & Eosin (H & E) and Goldner's trichrome to identify new bone formation. Three defects per group were used at each time point per analysis.

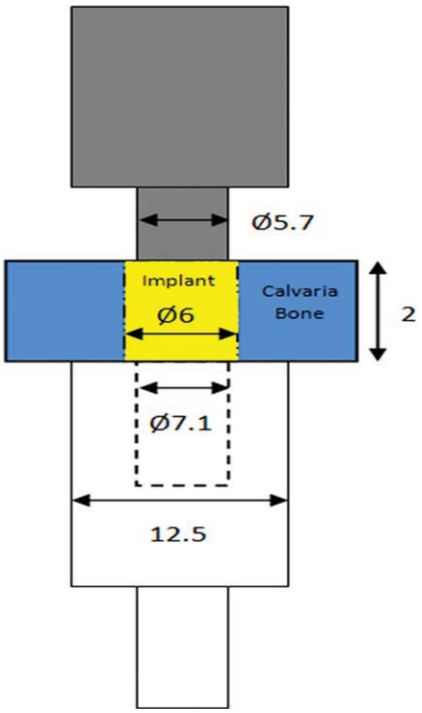

Figure 2. Schematic drawing of specimen undergoing push out test. [Color figure can be viewed in the online issue of this article, which is available at www.interscience.wiley.com.]

Statistical analysis

The mechanical testing (compressive strength and push out test), resultant scaffold volume loss and new bone formation values were presented as mean values ± the standard deviation (SD) of the mean. Data analyzes and comparisons were performed using Student's paired *t*-test (Microsoft Excel). *p*-values of <0.05 were considered as statistical significance.

RESULTS

All the rabbits used in the study remained healthy throughout the experiment and the healing was uneventful. All the scaffolds that were implanted within the assigned defects remained *in situ* with no signs of migration and rejection. There were also no reports of any adverse complications.

Gross morphological examination

All scaffolds demonstrated a smooth surface appearance and excellent integration with the surrounding native host bone (Fig. 3). In addition, all defect sites displayed complete closure without any signs of gaps of non-union. Majority of the scaffolds at 12 and 24 weeks displayed harmonious blending of the regenerated bone within the defect site with regards to color and texture. On palpation, the repaired sites were firm and stiff comparable to the adjacent host native bone. Numerous tiny blood vessels formation was observed within the newly regenerated PCL-TCP scaffolds in all three groups.

Mechanical testing

Compressive strength test

In this study, compressive strength was defined as the strength taken at 50% strain. Elastic modulus was taken at 79% strain as compared to at 1% strain normally to account for the uneven and irregular surface of the specimens.

The compressive strength of the various treatment groups of PCL-TCP scaffolds over the duration of implantation is shown in Figure 4. Generally, the NaOH treated groups showed superior compressive strength values primarily during the early phases of healing [2 weeks: Group A (4 ± 1.47 MPa), B (4.15 ± 1.43 MPa), C (5.15 ± 1.74 MPa); 4 weeks: Group A (5.92 ± 3.87 MPa), B (6.61 ± 3.6 MPa), C (9.86 ± 5.17 MPa); 8 weeks: Group A (7.92 ± 3.68 MPa), B (11.01 ± 5.51 MPa), C (15.11 ± 9.19 MPa)]. A decrease in compressive strength was reported in the later phases of healing throughout the three treatment groups. This reduction occurred earlier in the NaOH treated groups at 12 weeks as compared to the untreated group, which was observed later at 24 weeks.

Push out test

Figure 5 shows the push out test results of the various treatment groups of PCL-TCP scaffolds

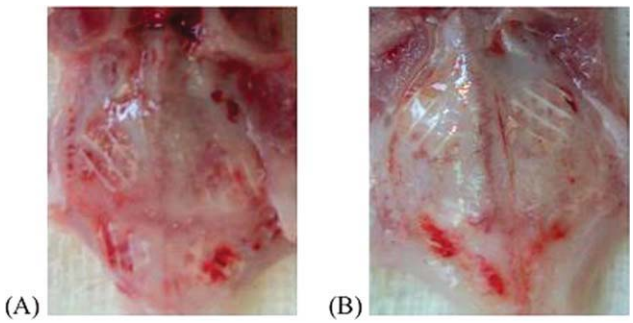

Figure 3. Gross photographs of the rabbit calvaria (A) 12 weeks and (B) 24 weeks following implantation of the scaffolds in the defects. The scaffolds were fully integrated into the surrounding host bone devoid of any fibrous encapsulation or foreign body reaction. Blood vessels formation were observed within all the reconstructed scaffolds. [Color figure can be viewed in the online issue of this article, which is available at www.interscience.wiley.com.]

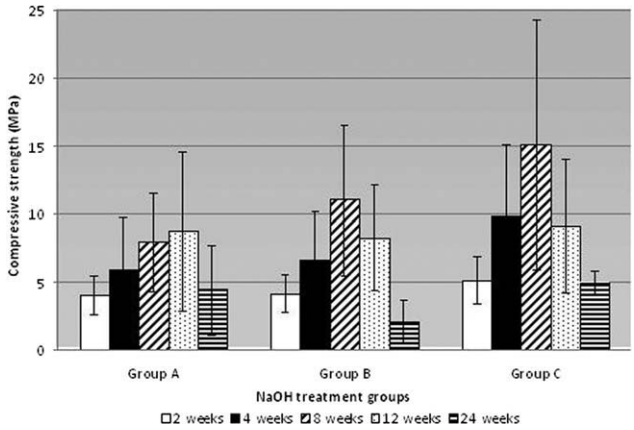

Figure 4. Compressive strength of PCL-TCP scaffolds under different NaOH treatment exposures over time. Data are shown as mean ± SD.

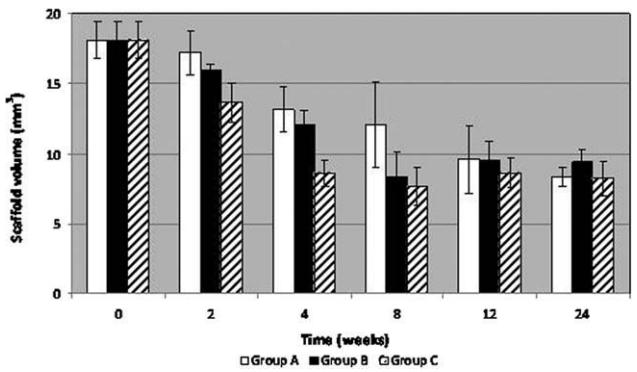

Figure 6. Resultant PCL-TCP scaffold volume under different NaOH treatment exposures over time. Data are shown as mean ± SD.

over the duration of implantation. Overall, increasing surface roughness of the scaffolds displayed a modest impact on the resultant push out test values of the treated scaffolds. Similar to the compressive strength results, a decrease in push out test values of the scaffolds was reported in the later phases of healing (12–24 weeks) in the NaOH treated groups, where only scaffolds from Group B showed a rebound in values. Scaffolds from the untreated group in general did not report any changes in the push out test values after 2 weeks following implantation.

Micro-CT analysis

Micro-CT was utilized to determine the cumulative loss of scaffold volume (Figs. 6 and 7) and the volume of new bone formation (Fig. 8) detected 2, 4, 8, 12, and 24 weeks after implantation. Results revealed that the gross honeycomb-like pattern of the interconnected pore network within the PCL-TCP scaffolds was generally maintained throughout the 24 weeks. However, signs of cracks and distortions were detected on the scaffold rods of the NaOH treated groups as early at 4 weeks. Figure 6 demonstrates the resultant scaffold volume detected at various time points for the different PCL-TCP scaffold groups. PCL-TCP scaffolds from all three groups measured a mean volume of 18.1 ± 1 mm^3 at the start of the experiment. In general, NaOH treated PCL-TCP scaffolds reported a more rapid breakdown as compared to the untreated ones during the early phases of healing (2–8 weeks). However, all three groups demonstrated comparable resultant scaffold volume at 12 and 24 weeks.

Surface modified scaffolds demonstrated a positive effect on the extent of degradation as they reported 50% scaffold volume losses earlier than the unmodified group. Scaffolds from Group C showed 50% degradation earliest around 4 weeks (8.6 ± 0.94

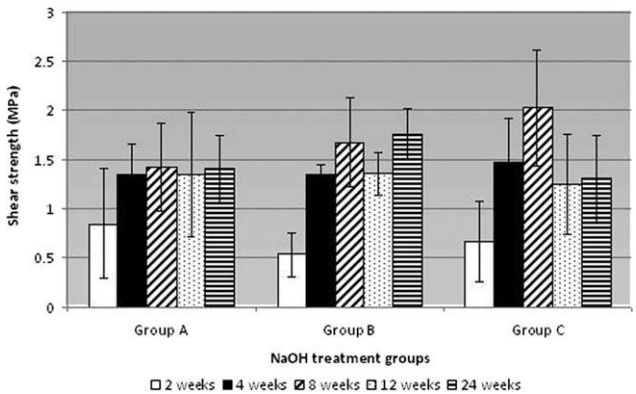

Figure 5. Push out test of PCL-TCP scaffolds under different NaOH treatment exposures over time. Data are shown as mean ± SD.

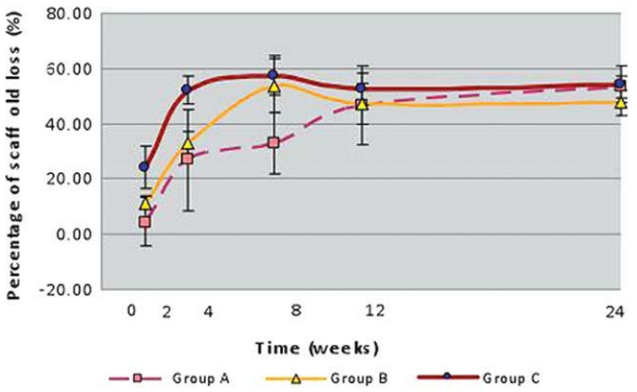

Figure 7. Percentage of PCL-TCP scaffold volume loss under different NaOH treatment exposures over time. Data are shown as mean ± SD. [Color figure can be viewed in the online issue of this article, which is available at www. interscience.wiley.com.]

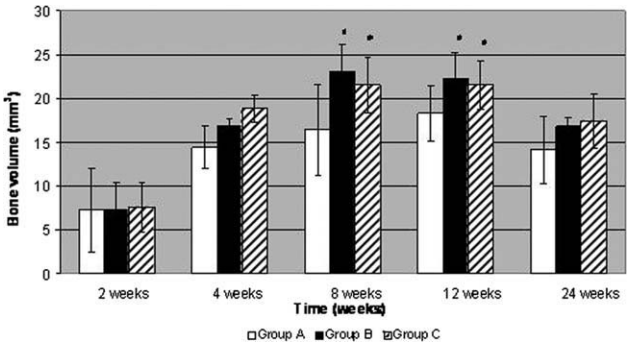

Figure 8. New bone formation within PCL-TCP scaffolds under different NaOH treatment exposures over time. Data are shown as mean ± SD. *Indicates statistical significant mean bone volume detected ($p < 0.05$) between untreated and NaOH treated scaffolds.

mm^3), Group B around 8 weeks (8.32 ± 1.79 mm^3) whilst Group A required ~12 weeks (9.6 ± 2.41 mm^3) before achieving similar outcomes (Fig. 7).

After the initial 2 weeks of implantation of the PCL-TCP scaffolds, micro-CT analysis showed superior new bone formation in the NaOH treated groups as compared to the untreated group throughout the 24 weeks. Significant increase in bone formation was detected after 8 and 12 weeks ($p < 0.05$). Across the three treatment groups, the volume of new bone formation reported the highest values between 8 and 12 weeks following implantation of the scaffolds [Group A (12 weeks): 18.29 ± 3.14 mm^3; Group B (8 weeks): 23.11 ± 3.11 mm^3; Group C (12 weeks): 21.51 ± 2.8 mm^3]. Interestingly, the amount of new bone formation detected at 24 weeks decreased accordingly whilst retaining a similar trend across the three treatment groups.

Histological analysis (Qualitative evaluation)

There was no evident distinction between the appearance and presentation of the scaffold across all the three treatment groups. There were no signs of generalized inflammatory activity or the formation of fibrous encapsulation in any of the histological specimens. Due to the process of histological preparations, the PCL-TCP scaffold was dissolved and in place represented as empty lacunae.

2 weeks (Fig. 9)

All defects, regardless of the scaffold treatment groups, demonstrated presence of a blood clot within the granulation tissue and fibrin matrix. Distinct arrangements of the scaffold rods were seen evenly distributed throughout the specimens. Interestingly, presence of obvious accumulation of inflammatory cells was detected in close proximity to the non-resorbable membrane; however, no signs of any inflammatory reaction were reported related to the scaffold material in all three treatment groups.

4 to 8 weeks (Fig. 10)

Considerable amount of bone formation were noted across all 3 treatment groups. Bone was seen infiltrating within the pores of the scaffold rods and

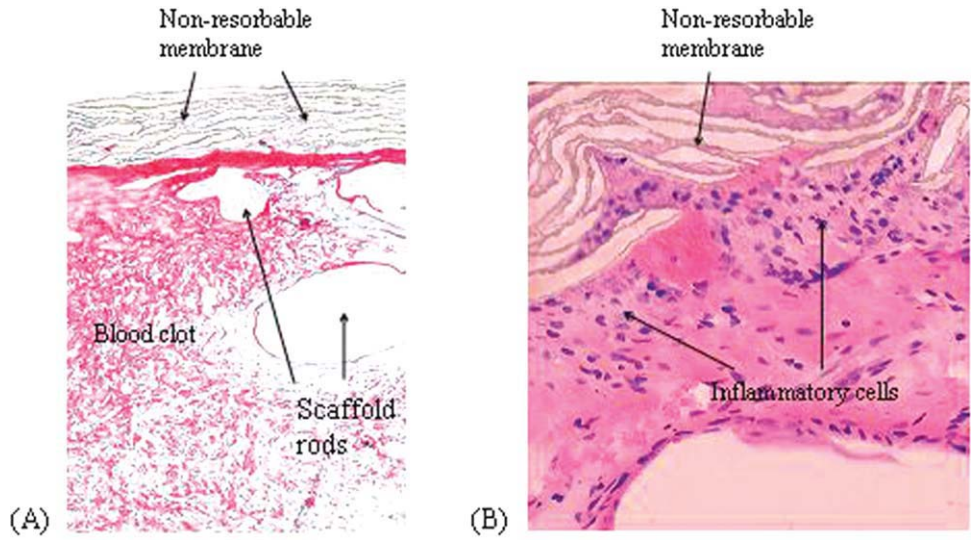

Figure 9. Representative histological images (H & E stain) of a PCL-TCP scaffold following implantation in the calvaria of a rabbit after 2 weeks. Note the generalized appearance of a blood clot within a fibrin network (A) (10× magnification) and the intense presence of inflammatory cells detected beneath the non-resorbable membrane (B) (40× magnification). [Color figure can be viewed in the online issue of this article, which is available at www.interscience.wiley.com.]

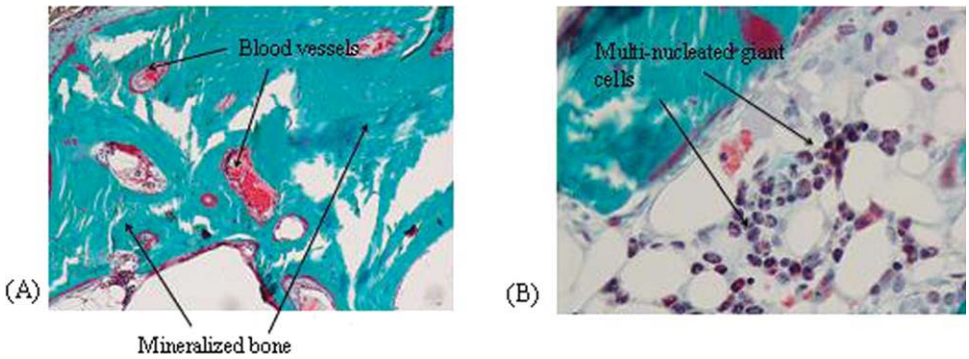

Figure 10. Goldner's trichrome staining (mineralized tissue = green; osteoid = red) reveals newly formed woven bone trabeculae after 4 weeks along with the presence of numerous blood vessels distributed across the defect site (A) (10× magnification). Multi-nucleated giant cells are detected on the surfaces of the scaffold rods and are closely associated with adipose cells as early as 4 weeks after implantation (B) (40× magnification).

along the surfaces of the scaffolds. Signs of bridging extending from the periphery of the host bone into the defect were noted. The deposition of bone presented as a slightly mature mineralized central portion and an outer region of newly formed and immature osteoid. In contrast to the 2 weeks' findings, a decrease in the amount of inflammatory cells was observed beneath the non-resorbable membrane; conversely, multinucleated osteoclast-like giant cells were increasingly detected on the surfaces of the scaffold rods and are closely associated with adipose cells. In addition, numerous vascular vessels were shown interspersed as well. Presence of an intense inflammatory reaction or a fibrous encapsulation related to the scaffolds was not detected.

12 to 24 weeks (Fig. 11)

The later phases of healing presented with increased fill of trabecular bone and adipose cell-rich bone marrow tissue surrounding the occasional scaffold rods throughout the entire defect space. Majority of the defect filled sites demonstrated a compact bone arrangement immediately beneath the non-resorbable membrane. The volume fraction of the adipose cell-rich bone marrow tissue was noted to have increased mainly at 24 weeks. Signs of an overt inflammatory reaction were absent in all specimens related to the scaffolds. In areas where multi-nucleated osteoclast-like giant cells were identified, they were often located on the surface of the scaffold rods that were intimately associated with adipose cell-rich bone marrow tissue.

DISCUSSION

Preliminary results from our earlier studies demonstrated that alkaline modification of PCL-TCP scaffolds improved surface properties and early bone formation. In this current study, a comprehen-

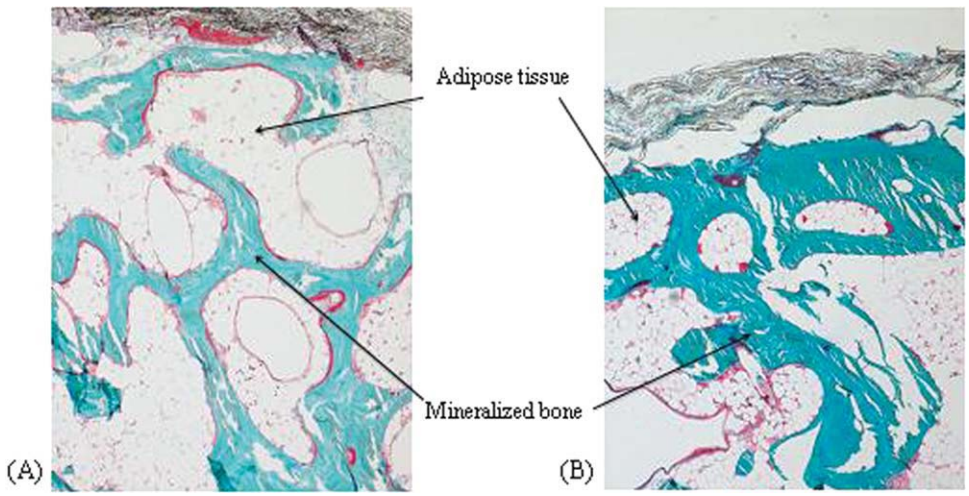

Figure 11. Goldner's trichrome staining (mineralized tissue = green; osteoid = red) reveals an increase in volume fraction of the adipose cell-rich bone marrow tissue was noted primarily after 24 weeks following implantation (A) (10× magnification) and (B) (5× magnification). Presence of blood vessels can be seen widely distributed across the defect specimens.

sive analysis was performed to investigate the degradation profile, mechanical properties and bone healing patterns of similarly modified PCL-TCP scaffolds over a period of 24 weeks in a rabbit calvaria defect model.

A rabbit calvaria defect model has been well established in the assessment of biomaterials targeted for bone regeneration applications.[1,22,23] Unlike majority of these studies, in which the critical-sized defects were used, the present study did not intend to utilize critical-sized defects to investigate the effects of surface modified PCL-TCP scaffolds. The objective of the study aimed to compare scaffolds with varying exposures intervals to NaOH treatment and to determine the effects on the degradation profile, biomechanical properties as well as the bone healing patterns. Alkaline treatment of PCL based scaffolds has been shown *in vitro* and *in vivo* to accelerate the degradation process through surface erosion and an increased exposed surface area for further hydrolytic chain scissions.[20,24] In addition, no reports of adverse host tissue reactions or cytotoxicity were favorably reported when NaOH pretreated PCL or PCL-TCP scaffolds were implanted in animal models.[21,24] Our recent study demonstrated that although NaOH treated PCL-TCP scaffolds displayed altered surface characteristics, there was no significant changes to the physical and structural characteristics. The overall pore dimensions and the ideal honeycomb interconnected remained intact.

Upon implantation of the treated and untreated PCL-TCP scaffolds, surface degradation and erosion commenced. This involved hydrolytic cleavage of the polymer backbone primarily at the surface and less into the bulk of the polymer without affecting the overall molecular weight, physical or chemical attributes. During the early phases of healing following implantation, the rate of scaffold volume loss was achieved faster in the NaOH treated groups than the untreated group. This was due to the increase in exposed surface areas that resulted initially from the formation of numerous microcavities and "channel-like" indentations on the scaffold rods after pretreatment with NaOH. Unlike the untreated PCL-TCP scaffolds, the treated ones displayed cleaved chains and oligomers that encouraged rapid clearance. However, the scaffold volume loss remained comparable during the later phases of healing, suggesting that once the superficial layer of the polymer had been removed after 12 weeks, the scaffold features were similar to that of the untreated and native PCL-TCP scaffolds.

Our assessment of bone healing patterns included micro-CT and histological analyzes. Micro-CT was employed to provide an accurate means to quantify bone and its spatial growth and three-dimensional distribution. Histology images were used to determine the qualitative aspects of bone formation, vascular, cellular and inflammatory activities. As expected from micro-CT data, scaffolds with increased surface roughness demonstrated superior bone formation as compared to the untreated group throughout the experiment. Histological analyzes over the progressive time points revealed increasing amounts of bone and adipose tissue infiltrating the pores in all scaffolds. In addition, numerous vascular vessels were seen interspersed within the regenerated defect sites. The presence of intense inflammatory cells or fibrous encapsulation was not detected. However, multinucleated osteoclast-like giant cells were identified in close approximation to the surface of the scaffold rods that were intimately associated with adipose cell-rich bone marrow tissue. It is important to note that these multinucleated osteoclast-like giant cells are primarily located on the surfaces of the PCL-TCP scaffold rods and do not demonstrate presence of any resorption lacunae on the newly formed bone as shown similar by other studies.[25–27] This is in accordance to the phenomenon that was described by Pogoda et al. as "functional coupling in the bone metabolic unit (BMU)."[28] It demonstrated the characteristics of the absence of osteoclast-associated resorption lacunae in the BMU and no quantitative reduction of bone volume. The multinucleated giant cells observed in the present study behaved primarily as macrophages, where the removal of graft particles would enable deposition of new bone to occur. Interestingly, a modest decrease in the overall bone volume was detected from micro-CT from 12 to 24 weeks (19.15–24.56%) across all the three treatment groups. Conversely, results from the histological analyzes demonstrated an increased volume fraction presence of adipose cell-rich bone marrow tissue surrounding the bony trabeculae. At this stage of healing, considerable remodeling of the bone could have occurred and adopted a cancellous nature.

The compressive test was conducted to investigate the mechanical integrity of the reconstructed scaffold-new bone composite. The push-out test was designed to examine the integration strength of the scaffold to the host bone of the calavria walls surrounding the defect. This was achieved by measuring the amount of strength required to fracture the reconstructed scaffold from the defect site. Results from the mechanical testing demonstrated a substantial variance in values. This was largely due to the differences in structural morphology, cross-sectional thickness and trabecular density of the rabbits' calvaria, despite controlling the age, gender of the rabbits and maintaining the size and positions of the defect sites. In general, mechanical testing results revealed improved values of the NaOH treated scaffolds as compared to the untreated scaffolds primarily dur-

ing the early phases of healing following implantation of the scaffolds. This proved favorable during the initial consolidation process of the implanted scaffolds where superior structural stability of the system was achieved as early as 8 weeks. Compressive strength analyzes reported a decrease in readings at the later stages of healing, in which on average closely matched to that of cancellous bone.[29,30] This findings corroborated with the earlier discussion from the histological data, in which the properties of the remodeled bone was suggested to have assumed a more cancellous type characteristic after initial bone healing had taken place. Due to the absence of load bearing forces in the calvaria region, our group proposed that during the later stages of healing, remodeling of bone occurred. This might result in a loss of bone mass and eventually adopt a less compact nature. The importance of mechanical loading for the maintenance and increase of bone mass was described early as the classic Wolff's Law[31] and is universally accepted today.[32] In addition, we believe that the clearance of the PCL-TCP polymer by the macrophages could encourage adipose clusters to be deposited. This was clearly reported in several of the studies that investigated the use of PCL-TCP scaffolds although it has yet to be proven.[1,18,24] Overall, the mechanical properties of both treated and untreated PCL-CTP scaffolds were shown to be favorable throughout the experiment, more importantly during the early phases of healing. This is essential especially in dentoalveolar applications where the oral cavity is constantly under the influence of moderate load bearing forces.

CONCLUSIONS

Selective surface modification of PCL-TCP scaffolds were implanted in calvaria defects of rabbits and evaluated for scaffold degradation, mechanical properties and patterns of bone formation. Throughout the experiment, scaffolds with increased surface roughness displayed encouraging results when new bone formation and mechanical properties were analyzed as compared to untreated and native ones. Based on the promising results from our rabbit study, we are currently in the process of investigating the potential of modified PCL-TCP scaffolds in a large animal model involving more challenging dentoalveolar defects. Here, a clinically relevant defect model will allow load-bearing forces to be taken into considerations in the oral cavity.

The authors would like to acknowledge the assistance of Dr. Amber Sawyyer from the Stem Cell and Tissue Repair Group, Institute of Medical Biology, Biopolis, Singapore for her invaluable support and advice.

References

1. Schantz J-T, Teoh SH, Lim TC, Endres M, Lam XFC, Hutmacher DW. Repair of calvarial defects with customized tissue-engineered bone grafts I. Evaluation of osteogenesis in a three-dimensional culture system. Tissue Eng 2003;9(Suppl 1):113–126.
2. Schantz J-T, Hutmacher DW, Lam XFC, Brinkmann M, Wong KM, Lim TC, Chou N, Guldberg RE, Teoh SH. Repair of calvarial defects with customized tissue-engineered bone grafts II. Evaluation of cellular efficiency and efficacy in vivo. Tissue Eng 2003;9(Suppl 1):127–139.
3. Rai B, Teoh SH, Ho KH, Hutmacher DW, Cao T, Chen F, Yacob K. The effect of rhBMP-2 onto 3D bioactive polycaprolactone scaffolds. Biomaterials 2004;25:5499–5506.
4. Rai B, Teoh SH, Hutmacher DW, Cao T, Ho KH. Novel PCL-based honeycomb scaffolds as drug delivery systems for rhBMP-2. Biomaterials 2005;26:3739–3748.
5. Rai B, Oest ME, Dupont KM, Ho KH, Teoh SH, Guldberg RE. Combination of platelet-rich plasma with polycaprolactone-tricalcium phosphate scaffolds for segmental bone defect repair. J Biomed Mater Res A 2007;81:888–899.
6. Rai B, Ho KH, Lei Y, Si-Hoe KM, Teo JCM, Yacob KB, Chen F, Ng FC, Teoh SH. Polycaprolactone-20% tricalcium phosphate scaffolds in combination with platelet-rich plasma for the treatment of critical-sized defects of the mandible: A pilot study. J Oral Maxillofac Surg 2007;65:2195–2205.
7. Jeong JC, Lee J, Cho K. Effects of crystalline microstructure on drug release behavior of poly (ε-caprolactone) microspheres. J Controlled Release 2003;92:249–258.
8. Hutmacher DW, Schantz T, Zein I, Ng KW, Teoh SH, Tan KC. Mechanical properties and cell cultural response of polycaprolactone scaffolds designed and fabricated via fused deposition modeling. J Biomed Mater Res 2001;55:203–216.
9. Lang NP, Brägger U, Hammerle CHF, Sutter F. Immediate transmucosal implants using the principle of guided tissue regeneration. I. Rationale, clinical procedures and 30-month results. Clin Oral Implant Res 1994a;5:154–163.
10. Lang NP, Hammerle CHF, Brägger U, Lehmann B, Nyman SR. Guided tissue regeneration in jaw bone defects prior to implant placement. Clin Oral Implant Res 1994b;5:92–97.
11. Du C, Cui FZ, Zhu XD, De Groot K. Three-dimensional nano-HAP/collagen matrix loading with osteogenic cells in organ culture. J Biomed Mater Res 1999;44:407–415.
12. Du C, Cui FZ, Feng QL, Zhu XD, De Groot K. Tissue response to nano-hydroxyapatite/collagen composite implants in marrow cavity. J Biomed Mater Res 1998;42:540–548.
13. Kay S, Thapa A, Haberstroh KM, Webster TJ. Nanostructured polymer/Nanophased ceramic composites enhance osteoblast and chondrocyte adhesion. Tissue Eng 2002;8: 753–761.
14. Liu H, Slamovich EB, Webster TJ. Increased osteoblast functions among nanophase titania/poly(lactide-*co*-glycolide) composites of the highest nanometer surface roughness. J Biomed Mater Res A 2006;78:798–807.
15. Degasne I, Basle MF, Demais V, Hure G, Lesourd M, Grolleau B, Mercier L, Chappard D. Effects of roughness, fibronectin and vitronectin on attachment, spreading, and proliferation of human osteoblast-like cells (Saos-2) on titanium surfaces. Calcif Tissue Int 1999;64:499–507.
16. Shapoff CA, Bowers GM, Levy B, Mellonig JT, Yukna RA. The effect of particle size on the osteogenic activity of composite grafts of allogenic freeze-dried bone and autogenous marrow. J Periodontol 1980;51:625–630.
17. Graziano A, D'aquino R, Cusella-De Angelis MG, Laino G, Piattelli A, Pacifici M, De Rosa A, Papaccio G. Concave pit-containing scaffold surfaces improve stem cell-derived osteoblast performance and lead to significant bone tissue formation. PLoS ONE 2007;2:e496.

18. Yeo A, Rai B, Sju E, Cheong JJ, Teoh SH. The degradation profile of novel, bioresorbable PCL-TCP scaffolds: An in vitro and in vivo study. J Biomed Mater Res A 2007;84:208–218.
19. Zein I, Hutmacher DW, Tan KC, Teoh SH. Fused deposition modeling of novel scaffold architectures for tissue engineering applications. Biomaterials 2002;23:1169–1185.
20. Yeo A, Sju E, Rai B, Teoh SH. Customizing the degradation and load-bearing profile of 3D polycaprolactone-tricalcium phosphate (PCL-TCP) scaffolds under enzymatic and hydrolytic conditions. J Biomed Mater Res B: Appl Biomater 2008;87:562–569.
21. Yeo A, Wong WJ, Khoo HH, Teoh SH. Surface modification of PCL-TCP scaffolds improve interfacial mechanical interlock and enhance early bone formation: An in vitro and in vivo characterization. J Biomed Mater Res A 2010;92:311–321.
22. Kroese-Deutman HC, Wolke JG, Spauwen PH, Jansen JA. Closing capacity of cranial bone defects using porous calcium phosphate cement implants in a rabbit animal model. J Biomed Mater Res A 2006;79:503–511.
23. Clokie CM, Moghadam H, Jackson MT, Sandor GK. Closure of critical sized defects with allogenic and alloplastic bone substitutes. J Craniofac Surg 2002;13:111–121.
24. Lam CX, Hutmacher DW, Schantz JT, Woodruff MA, Teoh SH. Evaluation of polycaprolactone scaffold degradation for 6 months in vitro and in vivo. J Biomed Mater Res A 2009;90:906–919.
25. Jensen SS, Aaboe M, Pinholt EM, Hjørting-Hansen E, Melsen F, Ruyter IE. Tissue reaction and material characteristics of four bone substitutes. Int J Oral Maxillofac Implants 1996;11:55–66.
26. Schlegel KA, Fichtner G, Schultze-Mosgau S, Wiltfang J. Histologic findings in sinus augmentation with autogenous bone chips versus a bovine bone substitute. Int J Oral Maxillofac Implants 2003;18:53–58.
27. Jensen SS, Broggini N, Hjørting-Hansen E, Schenk R, Buser D. Bone healing and graft resorption of autograft, anorganic bovine bone and β-tricalcium phosphate. A histologic and histomorphometric study in the mandibles of minipigs. Clin Oral Implants Res 2006;17:237–243.
28. Pogoda P, Priemel M, Rueger JM, Amling M. Bone remodeling: New aspects of a key process that controls skeletal maintenance and repair. Osteoporos Int 2005;16(Suppl 2):S18–S24.
29. Rezwan K, Chen QZ, Blaker JJ, Boccaccini AR. Biodegradable and bioactive porous polymer/inorganic composite scaffolds for bone tissue engineering. Biomaterials 2006;27: 3413–3431.
30. Rohl L, Larsen E, Lindhe F, Odgaard A, Jorgensen J. Tensile and compressive properties of cancellous bone. J Biomech 1991;24:1143–1149.
31. Wolff J. Das gesetz der Transformation der knochen. Berlin: Hirschwald; 1892.
32. Robling AG, Castillo AB, Turner CH. Biomechanical and molecular regulation of bone remodeling. Annu Rev Biomed Eng 2006;8:455–498.